Human Genetics (2019) 138:1275–1286
https://doi.org/10.1007/s00439-019-02068-8

ORIGINAL INVESTIGATION

Characterization of *GJB2 cis*-regulatory elements in the *DFNB1* locus

Stéphanie Moisan[1,2] · Anaïs Le Nabec[2] · Alicia Quillévéré[2] · Cédric Le Maréchal[1,2] · Claude Férec[1,2]

Received: 13 June 2019 / Accepted: 29 September 2019 / Published online: 4 October 2019

Abstract

Although most disease-causing variants are within coding region of genes, it is now well established that *cis*-acting regulatory sequences, depending on 3D-chromatin organization, are required for temporal and spatial control of gene expression. Disruptions of such regulatory elements and/or chromatin conformation are likely to play a critical role in human genetic disease. Hence, recurrent monoallelic cases, who present the most common hereditary type of nonsyndromic hearing loss (i.e., *DFNB1*), carry only one identified pathogenic allele. This strongly suggests the presence of uncharacterized distal *cis*-acting elements in the missing allele. Here within, we study the spatial organization of a large *DFNB1* locus encompassing the gap junction protein beta 2 (*GJB2*) gene, the most frequently mutated gene in this inherited hearing loss phenotype, with the chromosome conformation capture carbon copy technology (5C). By combining this approach with functional activity reporter assays and mapping of CCCTC-binding factor (CTCF) along the *DFNB1* locus, we identify a novel set of cooperating *GJB2 cis*-acting elements and suggest a *DFNB1* three-dimensional looping regulation model.

Introduction

Hearing loss affects 6–8% of the world's population including about 1 in 600 newborns (Morton and Nance 2006). It is estimated that almost 50% of this most common congenital sensory impairment in humans has a genetic origin (Shearer et al. 1993; Smith and Van Camp 1993). Nonsyndromic hearing loss (NSHL) represents 85% of hereditary deafness with over 100 genes associated. Syndromic hearing loss presenting other clinical signs with prelingual onset or postlingual onset (Roux et al. 2004) is related with even more genes (https://hereditaryhearingloss.org). Over 50% of autosomal-recessive NSHL results from pathogenic variants in the *DFNB1* locus (MIM #220290) (Smith and Van Camp 1993; Guilford et al. 1994). The gene most frequently mutated in inherited hearing loss, the gap junction protein beta 2 (*GJB2)* (MIM #121011), lies at the *DFNB1* locus on 13q12 (Zelante et al. 1997; Chan and Chang 2014). The *GJB2* gene is rather small (5513 bp) encompassing two exons (193 bp and 2141 bp long) separated by a 3179-bp intron (Kiang et al. 1997). The entire protein-coding sequence of 678 bp is located in the second exon which encodes 226 amino acids which corresponds to connexin 26 transmembrane protein (Cx26). The gap junction channel protein Cx26 is critical in intercellular communication among supporting cells and homeostasis of the cochlear, perilymph and endolymph fluids (Forge et al. 1999; Kikuchi et al. 2000). Cx26 is expressed in many cells in the whole body and especially within the human cochlea (Liu et al. 2009). In addition to over 200 *GJB2* mutations (http://deafnessvariationdatabase.org), six large deletions of the *DFNB1* locus have been reported as disease-causing mutation in NSHL (Stenson et al. 2017). Two deletions remove not only the entire *GJB2* gene but also another connexin gene *GJB6*, also located in the *DFNB1* locus at 5′ of *GJB2*; del-920 kb (Feldmann et al. 2009) and del-101 kb (*GJB2*-D13S175) (Bliznetz et al. 2017). Two other large deletions remove only the *GJB6* gene; del(*GJB6*-D13S1830) of 309 kb (Lerer et al. 2001; del Castillo et al. 2002; Pallares-Ruiz et al. 2002) and

Stéphanie Moisan and Anaïs Le Nabec contributed equally to this work and should be considered co-first authors.

Electronic supplementary material The online version of this article (https://doi.org/10.1007/s00439-019-02068-8) contains supplementary material, which is available to authorized users.

✉ Stéphanie Moisan
moisan.stephanie@hotmail.fr

✉ Claude Férec
claude.ferec@univ-brest.fr

[1] Laboratoire de Génétique Moléculaire et d'Histocompatibilité, CHRU de Brest, Bretagne, Brest, France

[2] Univ Brest, Inserm, EFS UMR 1078, GGB, 29200 Brest, France

del(*GJB6*-D13S1854) of 232 kb (del Castillo et al. 2005). Lastly, two other *DFNB1* deletions keep the *GJB2* and *GJB6* genes intact and have been identified in autosomal-recessive NSHL cases; del-131 kb (Wilch et al. 2010) and del-179 kb (Tayoun et al. 2016). Despite the most common deletions, *GJB6*-D13S1830 and *GJB6*-D13S1854 which remove only *GJB6* gene, it has been clearly described that deafness is not the result of *GJB6* loss but due to disruption of *GJB2* expression (Rodriguez-Paris and Schrijver 2009; Rodriguez-Paris et al. 2011). These large *DFNB1* deletions should encompass *cis*-regulatory elements essential for *GJB2* expression, and more precisely within a 95.4-kb common deleted region (Wilch et al. 2010).

Indeed, three-dimensional chromatin organization plays a key role on gene expression. Gene regulation depends on *cis*-regulatory elements which can interact with gene promoters by chromatin looping. Alteration of chromatin architecture and/or *cis*-acting elements can lead to *cis*-ruption disorder.

To prove this, we map chromatin organization with the chromosome conformation chromatin carbon copy (5C) technique to identify new *GJB2* regulatory elements. We recently used this approach to identify several *CFTR* (Moisan et al. 2016) and *PKD2* (Moisan et al. 2018) enhancers and now apply it here to a large region spanning the *DFNB1* locus. We identify several chromatin interactions with the *GJB2* promoter and demonstrate in parallel, using functional analysis with a reporter assay, that interacting regions significantly increase *GJB2* expression while another reduces it. Finally, through chromatin immunoprecipitation analyses, we suggest that these novel enhancer elements could be brought together through chromatin looping via the recruitment of CCCTC-binding factor (CTCF).

Materials and methods

Cell collection and culture

Human nasal epithelial cells (HNEC) from healthy control individuals were harvested using a sterile cytology brush (Gyneas, cat. no. 02-106). HNECs were collected by brushing the middle turbinate with backward–forward and rotatory movements and were placed in a collecting medium (Ham's F12 (Lonza) containing 1% Ultroser G (Pall, cat. no. 15950-17), and 1% antibiotic (PAA, cat. no. P11-002). Survival of the cells in this medium was preserved until 96 h at room temperature. HNECs were detached from the brush by vortexing and were washed three times with Dulbecco's modified Eagle medium (DMEM; Lonza) supplemented with decreasing antibiotic concentrations and a final wash with 1× phosphate buffered saline (PBS). Cell suspensions were centrifuged for 5 min at 2200*g* at 4 °C. The cell pellets were resuspended in a selected and optimized cell culture media of human airway epithelial cells (Airway Epithelial Cell Growth Medium; PromoCell) and cells were cultured following the manufacturer's instructions.

Normal human epidermal keratinocytes (NHEK) were isolated from the epidermis of the skin of adults undergoing surgery. Samples were aseptically collected and washed three times with 70% ethanol and PBS. Skin samples were then cut into small pieces and treated with dispase (25 U/ml Gibco, USA) overnight in air–liquid interface at 4 °C. The epidermis was separated from the dermis, and cells were dissociated with a trypsin–EDTA solution (LONZA) for 15 min. After filtration, cells were cultured in Keratinocyte Growth Medium (PromoCell).

Small airway epithelial cells (SAEC) were purchased from LGC Standards (lot No. 0234) and also grown in airway epithelial cell medium from PromoCell.

All cells were grown on plastic at liquid interface at 37 °C in 5% CO_2 saturated humid air.

GJB2 expression analysis by RT-PCR

Total RNA was extracted using RNeasy Plus mini kit (Qiagen) according to the manufacturer's instructions. Extracted RNA was eluted in RNase-free water and the concentration was determined using a nano-photometer (Implen GmbH, München, Germany). Reverse transcription was performed with 2 µg of total RNA using the SuperScript™ II Reverse Transcriptase kit (Life Technologies). PCR was performed with the HotStarTaq Polymerase (Qiagen) using two different pair of primers with the following primer sequences (5′–3′): a common GJB2 forward (1/2)-TTCCTCCCGACG CAGAGCAA, GJB2 reverse (1)-GGGCAATGCGTTAAA CTGGC and GJB2 reverse (2)-TCCTTTGCAGCCACAACG AGGAT, beta-actin forward-GTTGCTATCCAGGCTGTG and beta-actin reverse-CACTGTGTTGGCGTACAG.

Cell isolation and fixation for 5C analysis

HNEC cells were fixed with 1.5% formaldehyde for 10 min at room temperature. Crosslinking was stopped with glycine (125-mM final concentration), by incubating 5 min at room temperature followed with 15 min on ice. Cells were scraped and centrifuged at 400*g* for 10 min at 4 °C. Supernatants were removed and the cell pellets were quick-frozen on dry ice.

3C library preparation

The fixed HNEC cell pellets were treated as previously described (Dostie and Dekker 2007; Ferraiuolo et al. 2010). Briefly, 10 million cells were incubated in lysis buffer [10-mM Tris (pH 8.0), 10-mM NaCl, 0.2% NP-40, supplemented with fresh protease inhibitor cocktail] 10 min on ice. Cells

were then disrupted on ice with a Dounce homogenizer (pestle B; 2×20 strokes). Nuclei were recovered by centrifugation, washed twice with 1× *Eco*RI buffer (NEB) and resuspended in 100 µl of 1× *Hin*dIII buffer. 1× *Hin*dIII buffer (337 µl) was added to 50 µl of cell suspension, and the mixture was incubated for 10 min at 65 °C with 0.1% SDS final concentration (38 µl). Triton X-100 (44 µl of 10% Triton X-100) was added before overnight digestion with *Hin*dIII (400 U). The restriction enzyme was inactivated the next day by adding 86 µl of 10% SDS, and incubating 30 min at 65 °C. Samples were then individually diluted into 7.62 ml of ligation mix (750 µl of 10% Triton X-100, 750 µl of 10× ligation buffer, 80 µl of 10 mg/ml BSA, 80 µl of 100-mM ATP and 3000 Cohesive end Units of T4 DNA ligase). Ligation was carried out at 16 °C for 2 h. The 3C libraries were next incubated overnight with 45 µL of Proteinase K (10 mg/ml) at 55 °C. The DNA was purified by phenol–chloroform extraction and precipitated with 3-M NaOAc pH 5.2 (800 µl) and cold ethanol. After at least 1 h at − 80 °C, the DNA was recovered by centrifugation, the pellets were washed with cold 70% ethanol and then resuspended in 400 µl of 1× TE pH 8.0. A second phenol–chloroform extraction and precipitation with 3 M NaOAc pH 5.2 (40 µl) and cold ethanol were performed. DNA was recovered by centrifugation and washed eight times with cold 70% ethanol. The pellets were finally dissolved in 100 µl of 1× TE pH 8.0, and incubated with RNAse A (1 µl at 10 mg/ml) for 15 min at 37 °C.

5C primer and library design

5C primers covering the *DFNB1* region (hg19, chr13: 20,500,000-21,525,000), and two conserved chromatin compaction control regions: one within a house-keeping gene *ERCC3* (hg19, chr2:128,014,866–128,051,752) and another within the gene desert region *ENr313* (hg19, chr16:62,276,449–62,776,448) (Dostie et al. 2006) were designed using "my5C.primer" (Lajoie et al. 2009) and the following parameters: optimal primer length of 30 nt, optimal TM of 60 °C and default primer quality parameters (mer: 800, U-blast: 3, S-blasr: 50). Primers were not designed for large (> 20 kb) restriction fragments. Low complexity and repetitive sequences were excluded from our experimental design such that not all fragments could be probed in our assays. Primers with several genomic targets were also removed.

The universal A-key (CCATCTCATCCCTGCGTG TCTCCGACTCAG-(5C-specific)) and the P1-key tails ((5C-specific)-ATCACCGACTGCCCATAGAGAGG) were added to the Forward and Reverse 5C primers, respectively. Reverse 5C primers were phosphorylated at their 5′ ends. An anchored 5C design was used for the *DFNB1* locus, 1 Reverse 5C primers targeted the *GJB2* promoter while 49 Forward 5C primers covered the surrounding region.

For the control regions, an alternating 5C design was used: alternating Forward and Reverse 5C primers covering entire *ERCC3* and *ENr313* regions were used to generate the 5C libraries. This design used 41 primers (4 Forward/5 Reverse for the *ERCC3* region, 16 Forward/16 Reverse *ENr313* region). All 5C primer sequences are listed in Supplementary Table S1.

5C library preparation

5C libraries were prepared and amplified with the A-key and P1-key primers following a procedure described previously (Fraser et al. 2012). Briefly, 3C libraries were first titrated by PCR for quality control (single band, absence of primer dimers, etc.), and to verify that contacts were amplified at frequencies similar to what is usually obtained from comparable libraries (same DNA amount from the same species and karyotype) (Dostie and Dekker 2007; Dostie et al. 2007; Fraser et al. 2010).

5C primer stocks (20 µM) were diluted individually in water on ice, and mixed to a final concentration of 0.002 µM. Mixed primers were combined with annealing buffer (10× NEBuffer 4, New England Biolabs Inc.) on ice in reaction tubes. Salmon testis DNA was added to each 5C reaction, followed by the 3C libraries and water for a final volume of 10 µl. Samples were denatured at 95 °C for 5 min, and annealed at 50 °C for 16 h before ligation with Taq DNA ligase (10 U) for 1 h. Each ligation reaction was then PCR-amplified individually with primers against the A-key and P1-key primer tails. We used 35 cycles based on dilution series showing linear PCR amplification within that cycle range. The 5C PCR products of corresponding 3C libraries were pooled before purifying the DNA on MinElute columns (Qiagen).

5C libraries were quantified on agarose gel and diluted to 0.048 ng/µl. One microliter of diluted 5C library was used for sequencing with an Ion PGM™ sequencer. Samples were sequenced onto Ion 316™ Chips v2 following the Ion PGM Hi-Q Chef kit and Ion PGM™ Hi-Q Sequencing Kit protocols as recommended by the manufacturer's instructions (Thermo Fisher Scientific).

5C data analysis

Analysis of the 5C sequencing data was performed as described earlier (Fraser et al. 2012; Berlivet et al. 2013). The sequencing data were processed through a Torrent 5C data transformation pipeline on Galaxy as previously described (Fraser et al. 2012; Rousseau et al. 2014b) (http://galaxy.bci.mcgill.ca/galaxy/). This analysis generates an excel sheet containing interaction frequency lists (IFL) as well as a text file, which was used to visualize results using "my5C-heatmap" (Lajoie et al. 2009).

Normalization between different libraries was done first by read count and then using the compaction profiles for the *ERCC3* region and the gene desert region *ENr313*, setting one sample (HNEC) as a reference.

The *ERCC3* and *ENr313* 5C data of each sample were normalized by dividing the number of reads of each 5C contact by the total number of reads from the corresponding sequence run. A ratio, calculated by dividing these normalized data by normalized data from a reference sample (HNEC), was applied to the corresponding raw data of the study region for each sample.

Databases and URLs

The Hi-C data from human NHEK were downloaded from computational and functional Genomics/Epigenomics Yue Lab website at http://promoter.bx.psu.edu/hi-c/view.php. The Hi-C data shown in a heatmap format were binned at 25 kb. TAD and sub-TADs were outlined manually based on clustering of interaction frequencies.

DHS peaks, CTCF binding sites, H3K27Ac marks for SAEC and transcription factor ChIP-seq data of 161 factors from 91 cell types were obtained and visualized using UCSC genome browser (http://genome.ucsc.edu) (Kent et al. 2002).

The "my5C-primer" and "my5C-heatmap" bioinformatics tools are found at http://3dg.umassmed.edu/my5Cheatmap/heatmap.php.

Plasmid constructs

All the cloning steps were done using the "In fusion®" strategy from Clontech. Using the pGL3-Basic Vector (Promega), the 5′-flanking region of the *GJB2* gene (1541 bp, "P_{GJB2}") was cloned upstream from the firefly luciferase cDNA, at the *Hin*d III site. Candidate enhancer elements (A to D7′) were amplified and inserted downstream in the P_{GJB2} construct. All the inserted fragments were verified by sequencing. The PCR primers used to amplify the *GJB2* promoter, candidate enhancer sequences are shown in Supplementary Table S2.

Luciferase assay

1.25×10^5 cells were seeded in 12-well plates. Transfections were done 24 h later with the transit 2020 reagent (Mirus). 400 ng of the P_{GJB2} constructs and 100 ng of a pCMV-LacZ construct, as an internal control, were used for each condition. Every condition was done in triplicate. 48 h post-transfection, the cells were washed once with 1× PBS and lysed with Passive lysis buffer (Promega). Cells lysates were clarified by centrifugation at 12,000 *g* for 5 min at 4 °C. 20 µl of each protein extract were used to assay the luciferase activity and 25 µl for beta-galactosidase activity. We used Promega reagents and a multiwell plate reader Varioscan (Thermo Fisher). Results were presented as relative luciferase activity, with the P_{GJB2} construct activity equal to 1. Significance of the increased luciferase activity was performed using unpaired *t*-tests using GraphPad Prism® software.

Chromatin immunoprecipitation (ChIP) and qPCR

Formaldehyde (Sigma) was added to ~ 8.10^6 SAEC cells to obtain a final concentration of 1.5%. Crosslinking was allowed to proceed for 10 min at room temperature and stopped by the addition of glycine at a final concentration of 0.125 M. Fixed cells were washed and harvested with cold PBS. Chromatin was prepared following the SimpleChIP® Plus Enzymatic Chromatin IP protocol (Cell Signaling Technology) with minor modifications. The Adaptive Focused Acoustics™ (AFA) Technology from Covaris was used in addition to enzymatic digestion with micrococcal nuclease to produce DNA fragments of 150–900 bp. Chromatin was precleared with protein G agarose beads (Cell Signaling Technology) for 2 h at 4 °C and immunoprecipitate with 10 µL of CTCF-specific antibodies (Cell Signaling Technology #2899), a negative control IgG antibody or a positive control Histone H3 antibody (Cell Signaling Technology) was carried out overnight at 4 °C. Immune complexes were recovered by adding protein G agarose beads and incubated for 2 h at 4 °C. Beads were washed, DNA was eluted and crosslinks were reversed following the manufacturer's instructions. qPCR was performed in triplicate using QuantiTect SYBR® Green PCR Kit (Qiagen) in the Light Cycler 480 (Roche) and specific primers, as outlined in Supplementary Table S3. All immunoprecipitations were carried out at least in duplicate or even in triplicate to confirm the most significant sites, using different chromatin preparations. Results were presented as relative to CTCF-specific enrichment measured by dividing by the 2% input sample and subtracting the IgG-negative control signals.

Results

Chromatin organization of the human *DFNB1* locus

To pinpoint *cis*-acting regulatory elements at distance to *GJB2,* we map chromatin organization of the human *DFNB1* locus with the 5C technology and chose to conduct our analysis in primary human cells from healthy individuals. Primary cells provide most physiological *GJB2* expression levels and a normal karyotype in contrast to cell lines. GJB2 expression takes place in specific cell types in many different tissues. With the significant exception of hair cells, *GJB2* is expressed by nearly all cell types within the human cochlea, including supporting cells in the sensory epithelium,

fibrocytes and mesenchymal cells in the lateral wall, basal and intermediate cells of the stria vascularis and type I neurons in the spiral ganglion (Liu et al. 2009). Moreover, it has also been shown that *GJB2* is expressed in human and ferret airways and lung cells during development (Carson et al. 1998) and in normal sinus mucosa (Kim et al. 2016). Connexin proteins are enclosed in the plasma membrane and are involved in the function of the gap junctions between epithelial cells (BuSaba and Cunningham 2008). Consequently, and because there is no primary cell of the inner ear easily recoverable, we used primary human nasal epithelial cells (HNEC), small airway epithelial cells (SAEC) and normal human epidermal keratinocytes (NHEK) which have been described to well express *GJB2* (http://dnase.genome.duke.edu/geneDetail.php?ensemblID=gjb2) and for which we verified their expression (Fig. 1a).

To define more precisely the region where the *GJB2* promoter interactions are more susceptible, we used Hi-C data (Dixon et al. 2012, 2015). Hi-C is a high-throughput molecular technology, used to quantify all-to-all genome-wide chromosomal interactions in cell populations (Lieberman-Aiden et al. 2009). This technique demonstrated that the genome is organized into topologically associating domains (TADs) characterized by a much higher frequency of chromatin

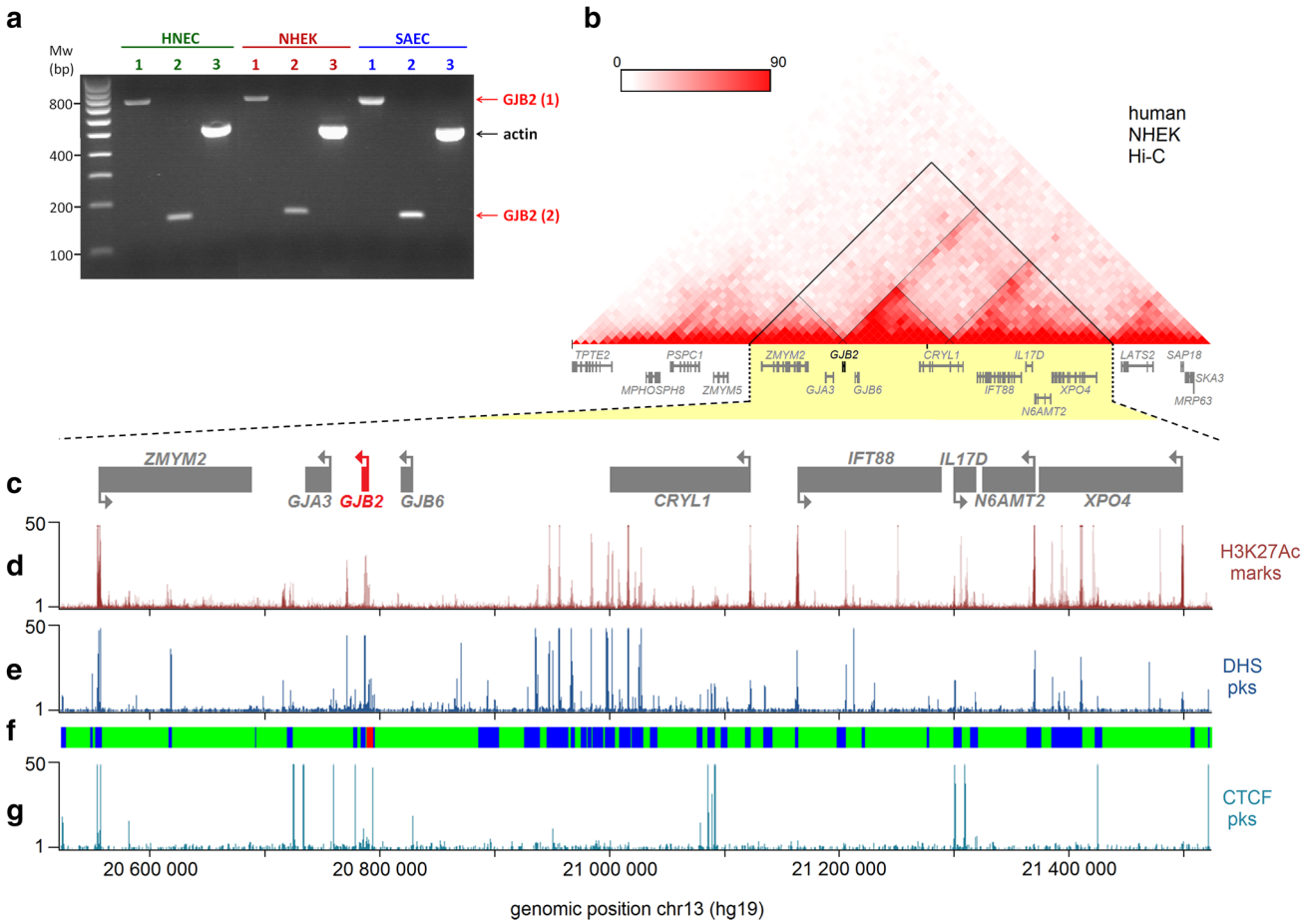

Fig. 1 Chromatin organization of the human *DFNB1* locus. **a** Endpoint RT-PCR analysis of *GJB2* expression in collected HNEC and NHEK samples, and in SAEC epithelial cells. Actin is shown as control for RNA integrity. **b** Hi-C data from NHEK human cells reveal that the *DFNB1* locus lies in a large TAD that contains several other genes (Dixon et al. 2012). *GJB2* is further contained within a sub-TAD. The Hi-C data are shown in heatmap form where increasing color intensity reflects higher interaction frequencies between genomic regions in 25-kb-resolution bins. Black lines outline the large TAD, while the dotted gray lines represent the sub-TADs. The genes contained within the area are shown under the heatmap. **c** Linear schematic representation of the ~1025 kb genomic region characterized in this study. Arrows indicate transcription orientation. The *GJB2* gene is shown in red and the neighboring genes in gray. **d** Alignment of H3K27Ac marks from 7 different cell lines over the region characterized. H3K27Ac peaks are often found near active regulatory elements. **e** Alignment of DNAseI hypersensitivity data from SAEC over the region characterized. DHS peaks identify open chromatin sites. **f** Anchored 5C primers design scheme used to map the genomic environment of the *DFNB1* locus and more precisely the *GJB2* promoter. A reverse "bait" 5C primer covering the *GJB2* promoter is shown in red. 49 Forward 5C primers shown in blue represent the rest of the locus. Green areas indicate regions not probed by 5C. 5C primer sequences are found in Supplementary Table S1. **g** Alignment of CTCF binding sites from SAEC over the area studied

contacts among these regions (Dixon et al. 2012; Nora et al. 2012).

TADs represent folded DNA regions, ranging in size between a few tens of kb to 3 megabases, which are largely conserved across cell types and species (Dekker et al. 2013; Dixon et al. 2016; Smith et al. 2016). TADs are delineated by boundaries enriched in CCCTC-binding factor (CTCF) sites (Rao et al. 2014). CTCF acts as a major protein driving chromatin looping, so the binding of CTCF may pinpoint regions that are important for tridimensional chromatin conformation organization. NHEK Hi-C data disclose that *GJB2,* displayed in black on the Fig. 1b, lies within a TAD spreading from before the *ZMYM2* until after the *XPO4* gene (Fig. 1b: black triangle). *GJA3*, another connexin genes not yet associated with hearing loss, itself localizes within a TAD substructure (sub-TAD, Fig. 1b: dotted triangle) centromeric to *GJB2*, (Phillips-Cremins and Corces 2013). *GJB2* itself is just localized between this sub-TAD and another which encompasses *GJB6* and a part of *CRYL1*. Based on these data, we designed our conformational analysis through a 1025-kb domain (hg19, chr13: 20,500,000–21,525,000) encompassing *DFNB1* connexin genes and their flanking genes: *ZMYM2* to *XPO4* (Fig. 1c).

We used 5C-seq to look for and quantify chromosomal regions interacting with the *GJB2* promoter (Dostie et al. 2006; Fraser et al. 2012). The 5C approach has previously been used to map chromatin organization and detect physical networks between promoters and regulatory elements (Sanyal et al. 2012; Berlivet et al. 2013; Phillips-Cremins et al. 2013). 5C starts with the production of a 3C library where a population of cells is fixed with formaldehyde to capture chromatin interactions. The fixed chromatin is then digested into fragments with a restriction enzyme, and a ligation step follows to generate pair-wise ligation products at frequencies reflecting physical proximity or accessibility between chromatin segments in vivo. The resulting 3C library is then converted into a 5C library by ligation-mediated amplification (LMA) where Forward and Reverse 5C primers are sequentially annealed and ligated at defined 3C junctions in a multiplex setting. The 5C ligation products are then amplified by PCR and processed for deep sequencing.

We designed 5C primers within our study locus to measure interaction frequencies between the *GJB2* promoter (one "bait" Reverse 5C primer in the promoter) and the sequence of the 1025-kb domain (49 Forward 5C primers) (Fig. 1f) according to some regulatory marks. Indeed, we only selected primers in regions displaying enhancer features using H3K27Ac marks from 7 different cell lines which are often found near active regulatory elements (Fig. 1d) and marker data available in SAECs. We looked particularly for the presence of DNase I hypersensitive sites (DHSs) (Fig. 1e) and for binding of CTCF (Fig. 1g) because they often reflect the presence of regulatory elements and since CTCF is a major protein driving the formation of chromatin loops genome-wide (Phillips and Corces 2009).

GJB2 promoter–chromatin interactions

We mapped the interaction profile of the *GJB2* promoter within the 1025-kb domain with 5C-seq in five HNEC samples (1–5) isolated from different healthy individuals (Fig. 2a,c). Whereas we collected several samples to avoid variation, variability is not unexpected in these kinds of data, particularly when comparing biological replicates where differences may be due from genetic variations among the donors, the overall transcription state of the cell populations, and the cell cycle distribution of the samples (Rousseau et al. 2014a). Notwithstanding these variabilities, we detect several chromatin contact peaks and particularly 4 regions that interact strongly with the *GJB2* promoter (highlighted in red boxes); one located downstream of the *GJB2* gene (Fig. 2c, "A") and three upstream (Fig. 2c, "B–D"). Interestingly, these long-range contacts with the *GJB2* promoter correspond to *DFNB1* chromatin regions inside several of the six large deletions associated with NSHL (Stenson et al. 2017) (Fig. 2b, c). The *GJB2* promoter chromatin contact peak "A" localizes in del-920 kb (Feldmann et al. 2009) and (*GJB2*-D13S175) (Bliznetz et al. 2017). Interaction regions "B" and "C" are not present in the del-101 kb but correlate with the other five deletions and more specifically partially encompass the 95.4-kb shared deleted region (highlighted in yellow in Fig. 2b, c). The farthest but nonetheless strongly interacting *GJB2* promoter contact, positioned about − 320 kb of the transcriptional start site of *GJB2* overlaps four of the six deletions: del-920 kb, del(*GJB6*-D13S1830) (Lerer et al. 2001; del Castillo et al. 2002; Pallares-Ruiz et al. 2002), del-179 kb (Tayoun et al. 2016) and del-131 kb (Wilch et al. 2010).

Accordingly, some of these *GJB2* promoter chromatin contacts present in large deletions of the *DFNB1* locus may correspond to DNA elements important for *GJB2* regulation.

Several distant DNA elements interacting with *GJB2* show *cis*-acting regulatory activities

To evaluate whether any of the *GJB2* identified looping regions act as functional *cis*-regulatory elements, we conducted enhancer activity tests in a reporter assay. Region C is not a unique 5C *Hin*dIII fragment with a single peak of interaction with the *GJB2* promoter fragment but a quite large DNA region enriched in chromatin contacts. To narrow down our analyses, we choose to focus on four candidate regions depending on their overlap with the higher DHS peaks from SAEC data (Fig. 3a, "C1–C4"). Similarly, the 5C *Hin*dIII fragment region D which gives the strongest interaction is too long to be cloned (5356 bp). As this region does

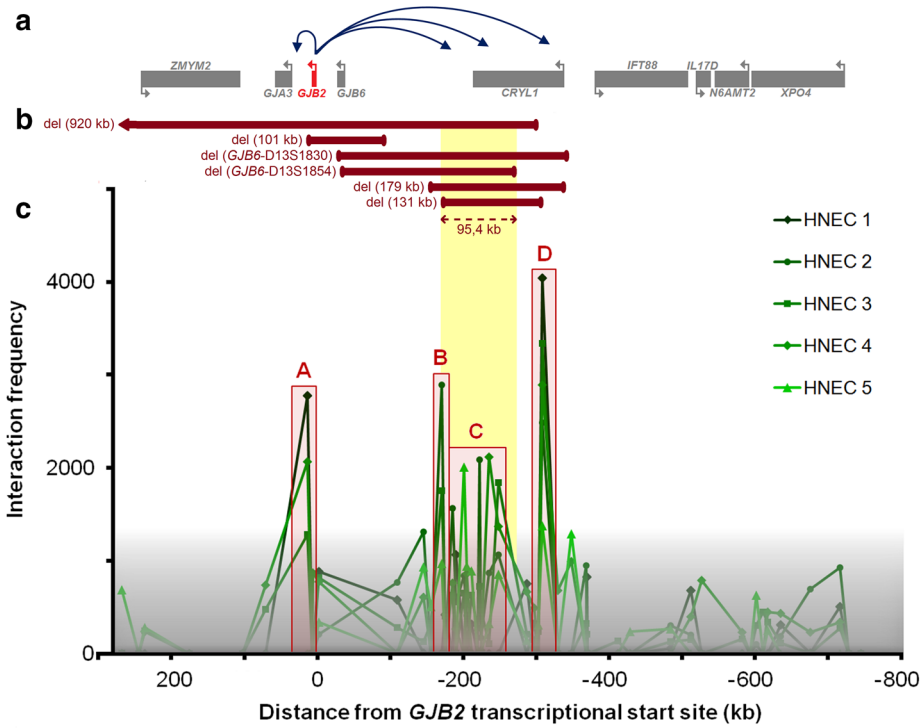

Fig. 2 *GJB2* promoter–chromatin interactions. **a** Schematic linear representation of the ~ 1025 kb *DFNB1* locus under study. **b** Summary of the six large deletions described at the *DFNB1* locus on chromosome 13q11-12. The proximal breakpoint of del(131 kb) and the distal breakpoint of del(*GJB6*-D13S1854) delimit the 95.4-kb common deleted region is represented by the yellow-highlighted area. **c** 5C chromatin interaction profiles of the *GJB2* promoter region in five HNEC samples. Interaction frequency (*y*-axis) is correlated with the position from the transcriptional start of *GJB2* (*x*-axis). Four strong contacting regions are highlighted in red boxes (A–D)

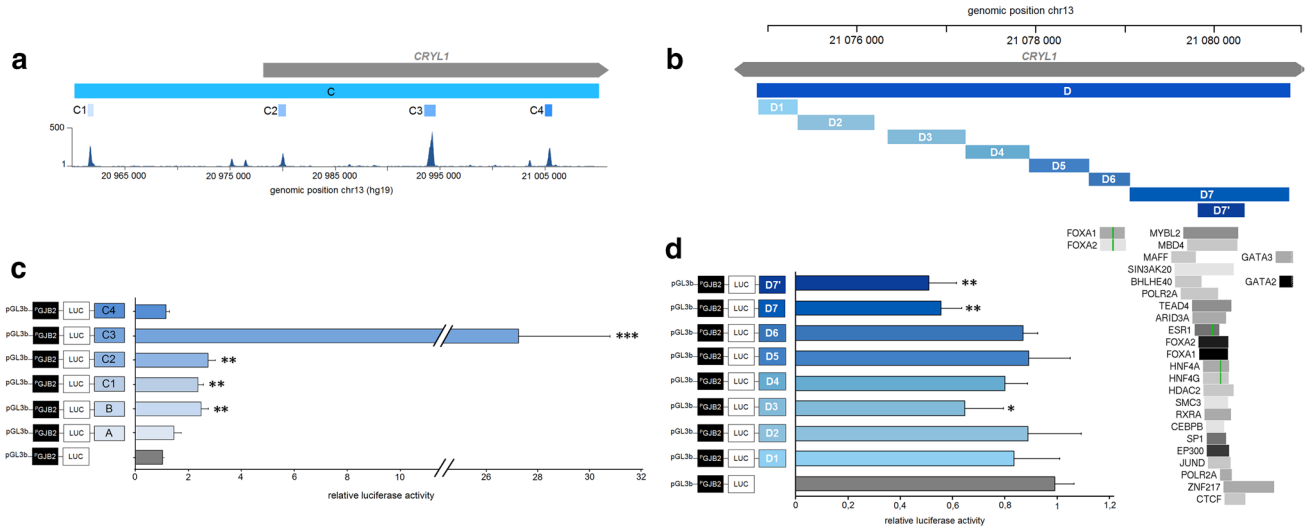

Fig. 3 *GJB2 cis*-acting regulatory elements. **a** Subsections of the region C into four candidate regions depending on their overlap with the higher DHS peaks from SAEC data. **b** Subsections of the 5C *Hin*dIII fragment D, which we originally found to interact with the *GJB2* promoter fragment, into eight candidate regions depending on their overlapping with several transcription factor or chromatin remodeler binding sites with Factorbook motifs identified by ChIP-seq in 91 different cell lines. **c**, **d** SAEC cells were transfected with pGL3B luciferase reporter constructs containing the *GJB2* basal promoter (P_{GJB2}; 1541 bp) and fragments of interacting *DFNB1* regions (A–D). Luciferase data are shown relative to the *GJB2* basal promoter vector (= 1). Error bars represent SEM ($n = 9$), $*P < 1.10^{-4}$/$**P < 1.10^{-9}$/$***P < 1.10^{-12}$ using unpaired t-tests

not encompass significant DHS sites, we decided to first study three candidate regions depending on their overlap with several transcription factor or chromatin remodeler binding sites with Factorbook motifs identified by ChIP-seq in 91 different cell lines (Fig. 3b, "D6, D7 and D7'"). Furthermore, whereas the 5′ segment of this region appears to be devoid of TF binding sites, it associates with a number of repeats, so we also examined this part of region D (Fig. 3b, "D1–D5").We first prepared a 'P_{GJB2}' construct by subcloning a 1541-bp *GJB2* promoter fragment into the

pGL3-Basic vector upstream of a modified firefly luciferase coding region optimized for analyzing transcriptional activity in eukaryotic cells. Fourteen candidate regions were then PCR amplified and inserted into P_{GJB2} (Supplementary Table S2). These different constructs were individually co-transfected into SAEC cells with a beta-galactosidase plasmid as a control for transfection efficiency. Firefly luciferase expression was measured after 48 h and was normalized against the P_{GJB2} construct alone, which was set to 1.

These tests reveal that our candidate regions act in different ways on *GJB2* promoter activity. Fragments encompassing regions B, C1, C2 significantly enhance *GJB2* expression with a modest effect of about two- to threefold increase of promoter activity, and fragment C3 has a strong gain of almost 27-fold (Fig. 3c). In contrast, three fragments of region D significantly reduce *GJB2* promoter activity, especially with the strongest effect of region D7′ which decrease *GJB2* expression twofold (Fig. 3d).

DFNB1 three-dimensional regulation looping model for *GJB2* gene expression

To better understand how these *cis*-acting elements participate to *GJB2* regulation, we looked for CTCF binding along *DFNB1* locus. To address this issue, we performed ChIP with a CTCF-specific antibody followed by quantitative PCR analysis with chromatin from SAEC. We examined fifteen CTCF binding sites along the *DFNB1* locus (Fig. 4a). These ChIP disclose only two sites that do not bind at all to CTCF factors (CTCF site 0 at proximity of the *GJB2* promoter and CTCF site at 61 kb of the TSS) but interestingly also present several specific CTCF sites enrichment. Particularly, these anti-CTCF ChIP show a ~ 3.5-fold enrichment of the 237 kb site, ~ 3-fold enrichment of the 34, 15 kb and − 298 kb sites. The − 727 kb upstream of the *GJB2* TSS site gave the most recruitment of CTCF with a ~ 5-fold enrichment (Fig. 4b). Interestingly, sites at 15 kb and − 298 kb of the *GJB2* TSS coincide with chromatin regions "A" and "D" which strongly interact with the *GJB2* promoter (Fig. 2c) and are located at boundaries of the sub-TAD which encompasses the *GJB2* and *GJB6* genes (Fig. 1b: dotted triangle). Sites at 237 kb and − 727 kb of the *GJB2* TSS correspond to functional

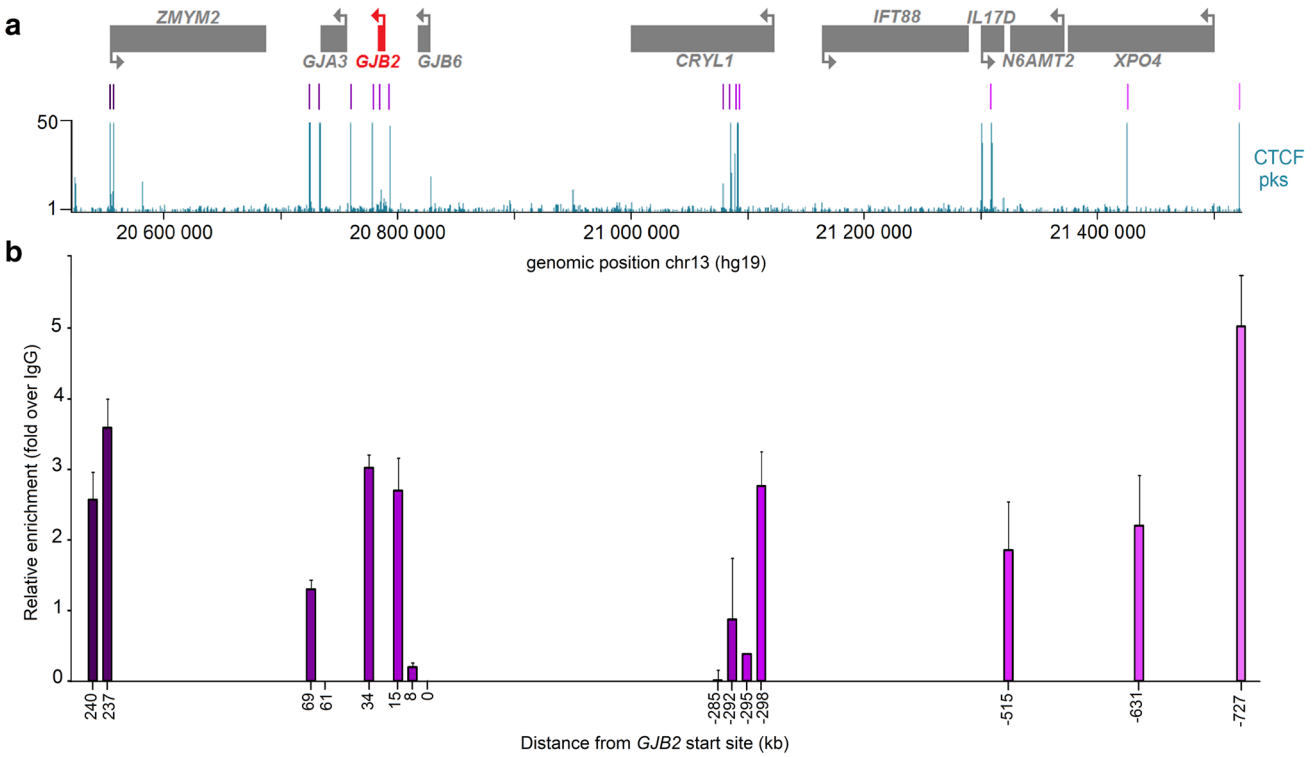

Fig. 4 Analysis of CTCF binding. **a** Alignment of CTCF binding sites from SAEC over the schematic linear representation of the region *DFNB1*. CTCF binding sites analyzed by ChIP-qPCR are indicated with purple lines. **b** Binding of CTCF at the *DFNB1* locus. Real-time PCR analysis of SAEC chromatin immunoprecipitated. Each value shown is relative to CTCF-specific enrichment measured with input and isotype-matched IgG-negative control. Error bars shown are S.E.M. qPCRs were performed in triplicate and immunoprecipitations were repeated at least two times and even three times at sites at 237 kb, 34 kb, 15 kb, − 292 kb, − 298 kb, − 515 kb and − 727 kb from the *GJB2* promoter

CTCF binding sites present on both sides of the large TAD spreading from before the *ZMYM2* until after the *XPO4* gene (Fig. 1b: black triangle).

All of these data provide a *DFNB1* three-dimensional regulation model for the *GJB2* gene expression. Indeed, recruitment of CTCF binding factors allows bringing of *cis*-acting elements to the *GJB2* promoter through chromatin looping. Enhancers from region C at more than 200 kb upstream from the *GJB2* TSS are certainly brought at proximity of *GJB2* promoter to activate it, thanks to a loop mediated by recruitment of CTCF factors on the sites at 15 kb and − 298 kb of the *GJB2* TSS. By contrast, these CTCF bindings strongly suggest the formation of a loop which acts as a barrier insulator element that avoids a repressor effect of region D located near − 310 kb of the *GJB2* TSS.

Discussion

Hearing impairment is a major trouble in our society and is at the heart of public health policies with nearly 10% of the general population affected. However, this invisible handicap remains poorly understood and overlooked. With about 50% of inherited forms, deciphering the precise regulatory characteristics of the human genome is a significant challenge to explain patient's case. We decided to focus our research on the *GJB2* gene, the gene most frequently mutated in hereditary hearing loss. While several studies suggest the presence of *cis*-regulatory elements of *GJB2*, to date, none of them have yet been characterized (Wilch et al. 2010). Thus, here we studied the spatial chromatin organization of a large *DFNB1* sequence over 1 Mb encompassing the *GJB2* gene with the chromosome conformation chromatin carbon copy (5C) technique to identify potential regulatory elements. This method was already successfully used to identify *CFTR* and *PKD2 cis*-acting elements (Moisan et al. 2016, 2018). Our three-dimensional *DFNB1* chromatin analyses reveal that several regions are at physical proximity of the *GJB2* promoter and especially four regions are engaged in strong interactions. Interestingly, these *GJB2* DNA contacts overlap with one or more of the six large deletions of the *DFNB1* locus suspected to contain regulatory elements (Wilch et al. 2010). From these interacting regions, nine fragments were tested for enhancer activity in reporter assays. In this way, our study enables characterization of several *GJB2 cis*-acting elements. Four enhancer regions significantly increase *GJB2* expression, three located at − 162 kb, − 190 kb, − 208 kb of the transcriptional start site (TSS) act modestly with a two- to threefold effect and another at − 222 kb has a stronger 27-fold effect. These enhancers are localized in the 95.4-kb commonly deleted region. The regulatory element located at − 309 kb of the TSS is not in the common *DFNB1* deleted region, and conversely has a repressor effect of a twofold decrease of *GJB2* activity. Finally, we studied binding of CTCF along the *DFNB1* locus by ChIP-qPCR. We identify several strong CTCF recruitments and describe four preferential sites. One is located just downstream of the *GJB2* gene at 15 kb, another upstream at − 298 kb and these two sites coincide with boundaries of a sub-TAD encompassing *GJB2* gene. A third binds at 237 kb and a last far away at − 727 kb of the *GJB2* TSS and occur, respectively, in the start and the end of the large TAD spreading from before the *ZMYM2* until after the *XPO4* gene of the *DFNB1* locus.

In conclusion, with these data, we identified a novel set of cooperating *cis*-acting elements that are associated with the regulation of *GJB2* expression and suggest a *DFNB1* three-dimensional looping model. CTCF–CTCF insulator bindings around the *GJB2* gene may organize the higher order structure of the chromatin and establish transcriptional active domains (Kim et al. 2007; Giles et al. 2010). A loop chromatin forming, which corresponds to the *GJB2* sub-TAD, not only would allow enhancers to be brought closer to the *GJB2* promoter, but also could avoid *GJB2* silencing with a possible enhancer-blocking insulator activity (Gaszner and Felsenfeld 2006; Chetverina et al. 2014). Thus, and because there is no available cell of the inner ear recoverable, these data from the most relevant cellular models provide, for the first time, valuable information on the basic insights of the regulation of *GJB2* gene.

Although most genetic disorders are caused by disease-causing variants within the coding region or splice site sequences of genes, it is now well established that pathogenic variants can be found within the 98% of non-coding DNA of the human genome (Boyle et al. 2012; Spielmann and Mundlos 2013, 2016). More precisely, distant *cis*-acting regulatory variants like variations in enhancer or insulator sequences can influence the 3D-genomic organization which modify the chromatin accessibility, and therefore alter gene expression (Epstein 2009; Kleinjan and Coutinho 2009; Crutchley et al. 2010).

Currently, the EMQN DFNB1 guidelines (Hoefsloot et al. 2013) recommend a genomic *DFNB1* testing based on sequencing of the *GJB2* gene and research of the two common deletions (*GJB6*-D13S1830 and *GJB6*-D13S1854). However, this diagnostic achieves highest detection rates in autosomal-recessive NSHL, with about 20% of the cases related to *DFNB1* with several of them being only monoallelic with an inconclusive genotype. Even if the main mutation (i.e., c.35delG) in the Caucasian population has a high carrier frequency of around 2% within the overall population, there is an excess among patients which suggests the involvement of an additional unidentified causal variant (Wilcox et al. 2000; Roux et al. 2004; Pollak et al. 2008; Leclère et al. 2017). This finding suggests that *cis*-acting regulatory elements for *GJB2* may exist at distance and will be removed within the large deletions. Single-nucleotide variants or structural variations at

distance could constitute the 'missing' mutation (Wilch et al. 2010). Variation within regulatory elements can account for quantitative different expression of alleles and may be partially responsible for some phenotypic variations (Azaiez et al. 2004; Marlin et al. 2005; Snoeckx et al. 2005; Hilgert et al. 2009) and could be explain possible presbycusis predisposition (Rodriguez-Paris et al. 2008; Wu et al. 2014; Fetoni et al. 2018).

Future studies will be aimed to more precisely describe these effects with CRISPR analyses, understanding the precise mechanisms by which *GJB2* expression is regulated by the characterization of cell-type-specific trans-acting factors and identifying variants in the *GJB2 cis*-regulatory elements that we have described. Private variants could be identified or structural variants might also be implicated (Sanchis-Juan et al. 2018). Unprecedented, *DFNB1* hearing loss may be associated with a *cis*-ruption disorder with the dysfunction of a *cis*-regulatory element (Kleinjan and Coutinho 2009).

Furthermore, characterization of *GJB2 cis*-acting elements will not only provide basic insights into the understanding of long-range regulation mechanisms of this gene, but also may be important for genetic diagnosis, refining genotype–phenotype correlations and thus to improve genetic counseling and therapy development and treatment of patients with NSHL.

Acknowledgements This work was supported by grants from the French foundation "La Fondation pour l'Audition", the "Région Bretagne" and the association "Gaétan Salaün". We thank Pr Laurent Misery and its team for keratinocytes. We are grateful to the members of Josée Dostie Lab for access to their Torrent 5C data transformation pipeline on Galaxy and for their excellent technical assistance. We thank Anthony Herzig for grammatical/editorial English corrections of this manuscript.

Author contributions SM: Designed and supervised the study, carried out the experiments, analyzed the data, wrote the paper. ALN: Carried out luciferase assays and ChIP experiments, analyzed the data. AQ: Carried out 5C experiments, analyzed the data. CLM: Edited the paper. CF: Supervised lab work, edited the paper. All authors read and approved the manuscript.

Data availability statement All data generated during this study are included in this published article and the supplementary files. The 5C datasets generated during the current study are available in the GEO databases: 5C-Seq data: Gene Expression Omnibus GSE128881 (https://www.ncbi.nlm.nih.gov/geo/query/acc.cgi?acc=GSE128881).

Compliance with ethical standards

Conflict of interest The authors declare that they have no conflict of interest.

References

Azaiez H, Chamberlin GP, Fischer SM, Welp CL, Prasad SD, Taggart RT, Del Castillo I, Van Camp G, Smith RJ (2004) GJB2: the spectrum of deafness-causing allele variants and their phenotype. Hum Mutat 24:305–311

Berlivet S, Paquette D, Dumouchel A, Langlais D, Dostie J, Kmita M (2013) Clustering of tissue-specific sub-TADs accompanies the regulation of HoxA genes in developing limbs. PLoS Genet 9:e1004018

Bliznetz EA, Lalayants MR, Markova TG, Balanovsky OP, Balanovska EV, Skhalyakho RA, Pocheshkhova EA, Nikitina NV, Voronin SV, Kudryashova EK, Glotov OS, Polyakov AV (2017) Update of the GJB2/DFNB1 mutation spectrum in Russia: a founder Ingush mutation del(GJB2-D13S175) is the most frequent among other large deletions. J Hum Genet 62:789–795

Boyle AP, Hong EL, Hariharan M, Cheng Y, Schaub MA, Kasowski M, Karczewski KJ, Park J, Hitz BC, Weng S, Cherry JM, Snyder M (2012) Annotation of functional variation in personal genomes using RegulomeDB. Genome Res 22:1790–1797

Busaba NY, Cunningham MJ (2008) Connexin 26 and 30 genes mutations in patients with chronic rhinosinusitis. Laryngoscope 118:310–313

Carson JL, Reed W, Moats-Staats BM, Brighton LE, Gambling TM, Hu SC, Collier AM (1998) Connexin 26 expression in human and ferret airways and lung during development. Am J Respir Cell Mol Biol 18:111–119

Chan DK, Chang KW (2014) GJB2-associated hearing loss: systematic review of worldwide prevalence, genotype, and auditory phenotype. Laryngoscope 124:E34–E53

Chetverina D, Aoki T, Erokhin M, Georgiev P, Schedl P (2014) Making connections: insulators organize eukaryotic chromosomes into independent cis-regulatory networks. BioEssays 36:163–172

Crutchley JL, Wang XQ, Ferraiuolo MA, Dostie J (2010) Chromatin conformation signatures: ideal human disease biomarkers? Biomark Med 4:611–629

Dekker J, Marti-Renom MA, Mirny LA (2013) Exploring the three-dimensional organization of genomes: interpreting chromatin interaction data. Nat Rev Genet 14:390–403

Del Castillo I, Villamar M, Moreno-Pelayo MA, Del Castillo FJ, Alvarez A, Telleria D, Menendez I, Moreno F (2002) A deletion involving the connexin 30 gene in nonsyndromic hearing impairment. N Engl J Med 346:243–249

Del Castillo FJ, Rodriguez-Ballesteros M, Alvarez A, Hutchin T, Leonardi E, De Oliveira CA, Azaiez H, Brownstein Z, Avenarius MR, Marlin S, Pandya A, Shahin H, Siemering KR, Weil D, Wuyts W, Aguirre LA, Martin Y, Moreno-Pelayo MA, Villamar M, Avraham KB, Dahl HH, Kanaan M, Nance WE, Petit C, Smith RJ, Van Camp G, Sartorato EL, Murgia A, Moreno F, Del Castillo I (2005) A novel deletion involving the connexin-30 gene, del(GJB6-d13s1854), found in trans with mutations in the GJB2 gene (connexin-26) in subjects with DFNB1 non-syndromic hearing impairment. J Med Genet 42:588–594

Dixon JR, Selvaraj S, Yue F, Kim A, Li Y, Shen Y, Hu M, Liu JS, Ren B (2012) Topological domains in mammalian genomes identified by analysis of chromatin interactions. Nature 485:376–380

Dixon JR, Jung I, Selvaraj S, Shen Y, Antosiewicz-Bourget JE, Lee AY, Ye Z, Kim A, Rajagopal N, Xie W, Diao Y, Liang J, Zhao H, Lobanenkov VV, Ecker JR, Thomson JA, Ren B (2015) Chromatin architecture reorganization during stem cell differentiation. Nature 518:331–336

Dixon JR, Gorkin DU, Ren B (2016) Chromatin domains: the unit of chromosome organization. Mol Cell 62:668–680

Dostie J, Dekker J (2007) Mapping networks of physical interactions between genomic elements using 5C technology. Nat Protoc 2:988–1002

Dostie J, Richmond TA, Arnaout RA, Selzer RR, Lee WL, Honan TA, Rubio ED, Krumm A, Lamb J, Nusbaum C, Green RD, Dekker J (2006) Chromosome conformation capture carbon copy (5C): a massively parallel solution for mapping interactions between genomic elements. Genome Res 16:1299–1309

Dostie J, Zhan Y, Dekker J (2007) Chromosome conformation capture carbon copy technology. Curr Protoc Mol Biol **(Chapter 21, Unit 21 14)**

Epstein DJ (2009) Cis-regulatory mutations in human disease. Brief Funct Genom Proteom 8:310–316

Feldmann D, Le Marechal C, Jonard L, Thierry P, Czajka C, Couderc R, Ferec C, Denoyelle F, Marlin S, Fellmann F (2009) A new large deletion in the DFNB1 locus causes nonsyndromic hearing loss. Eur J Med Genet 52:195–200

Ferraiuolo MA, Rousseau M, Miyamoto C, Shenker S, Wang XQ, Nadler M, Blanchette M, Dostie J (2010) The three-dimensional architecture of Hox cluster silencing. Nucleic Acids Res 38:7472–7484

Fetoni AR, Zorzi V, Paciello F, Ziraldo G, Peres C, Raspa M, Scavizzi F, Salvatore AM, Crispino G, Tognola G, Gentile G, Spampinato AG, Cuccaro D, Guarnaccia M, Morello G, Van Camp G, Fransen E, Brumat M, Girotto G, Paludetti G, Gasparini P, Cavallaro S, Mammano F (2018) Cx26 partial loss causes accelerated presbycusis by redox imbalance and dysregulation of Nfr2 pathway. Redox Biol 19:301–317

Forge A, Becker D, Casalotti S, Edwards J, Evans WH, Lench N, Souter M (1999) Gap junctions and connexin expression in the inner ear. Novartis Found Symp 219:134–150 **(discussion 151–136)**

Fraser J, Rousseau M, Blanchette M, Dostie J (2010) Computing chromosome conformation. Methods Mol Biol 674:251–268

Fraser J, Ethier SD, Miura H, Dostie J (2012) A Torrent of data: mapping chromatin organization using 5C and high-throughput sequencing. Methods Enzymol 513:113–141

Gaszner M, Felsenfeld G (2006) Insulators: exploiting transcriptional and epigenetic mechanisms. Nat Rev Genet 7:703–713

Giles KE, Gowher H, Ghirlando R, Jin C, Felsenfeld G (2010) Chromatin boundaries, insulators, and long-range interactions in the nucleus. Cold Spring Harb Symp Quant Biol 75:79–85

Guilford P, Ben Arab S, Blanchard S, Levilliers J, Weissenbach J, Belkahia A, Petit C (1994) A non-syndrome form of neurosensory, recessive deafness maps to the pericentromeric region of chromosome 13q. Nat Genet 6:24–28

Hilgert N, Huentelman MJ, Thorburn AQ, Fransen E, Dieltjens N, Mueller-Malesinska M, Pollak A, Skorka A, Waligora J, Ploski R, Castorina P, Primignani P, Ambrosetti U, Murgia A, Orzan E, Pandya A, Arnos K, Norris V, Seeman P, Janousek P, Feldmann D, Marlin S, Denoyelle F, Nishimura CJ, Janecke A, Nekahm-Heis D, Martini A, Mennucci E, Toth T, Sziklai I, Del Castillo I, Moreno F, Petersen MB, Iliadou V, Tekin M, Incesulu A, Nowakowska E, Bal J, Van De Heyning P, Roux AF, Blanchet C, Goizet C, Lancelot G, Fialho G, Caria H, Liu XZ, Xiaomei O, Govaerts P, Gronskov K, Hostmark K, Frei K, Dhooge I, Vlaeminck S, Kunstmann E, Van Laer L, Smith RJ, Van Camp G (2009) Phenotypic variability of patients homozygous for the GJB2 mutation 35delG cannot be explained by the influence of one major modifier gene. Eur J Hum Genet 17:517–524

Hoefsloot LH, Roux AF, Bitner-Glindzicz M (2013) EMQN Best Practice guidelines for diagnostic testing of mutations causing non-syndromic hearing impairment at the DFNB1 locus. Eur J Hum Genet 21:1325–1329

Kent WJ, Sugnet CW, Furey TS, Roskin KM, Pringle TH, Zahler AM, Haussler D (2002) The human genome browser at UCSC. Genome Res 12:996–1006

Kiang DT, Jin N, Tu ZJ, Lin HH (1997) Upstream genomic sequence of the human connexin26 gene. Gene 199:165–171

Kikuchi T, Kimura RS, Paul DL, Takasaka T, Adams JC (2000) Gap junction systems in the mammalian cochlea. Brain Res Brain Res Rev 32:163–166

Kim TH, Abdullaev ZK, Smith AD, Ching KA, Loukinov DI, Green RD, Zhang MQ, Lobanenkov VV, Ren B (2007) Analysis of the vertebrate insulator protein CTCF-binding sites in the human genome. Cell 128:1231–1245

Kim R, Chang G, Hu R, Phillips A, Douglas R (2016) Connexin gap junction channels and chronic rhinosinusitis. Int Forum Allergy Rhinol 6:611–617

Kleinjan DJ, Coutinho P (2009) Cis-ruption mechanisms: disruption of cis-regulatory control as a cause of human genetic disease. Brief Funct Genom Proteom 8:317–332

Lajoie BR, Van Berkum NL, Sanyal A, Dekker J (2009) My5C: web tools for chromosome conformation capture studies. Nat Methods 6:690–691

Leclère J-C, Le Gac M-S, Le Maréchal C, Ferec C, Marianowski R (2017) GJB2 mutations: genotypic and phenotypic correlation in a cohort of 690 hearing-impaired patients, toward a new mutation? Int J Pediatr Otorhinolaryngol 102:80–85

Lerer I, Sagi M, Ben-Neriah Z, Wang T, Levi H, Abeliovich D (2001) A deletion mutation in GJB6 cooperating with a GJB2 mutation in trans in non-syndromic deafness: a novel founder mutation in Ashkenazi Jews. Hum Mutat 18:460

Lieberman-Aiden E, Van Berkum NL, Williams L, Imakaev M, Ragoczy T, Telling A, Amit I, Lajoie BR, Sabo PJ, Dorschner MO, Sandstrom R, Bernstein B, Bender MA, Groudine M, Gnirke A, Stamatoyannopoulos J, Mirny LA, Lander ES, Dekker J (2009) Comprehensive mapping of long-range interactions reveals folding principles of the human genome. Science 326:289–293

Liu W, Boström M, Kinnefors A, Rask-Andersen H (2009) Unique expression of connexins in the human cochlea. Hear Res 250:55–62

Marlin S, Feldmann D, Blons H, Loundon N, Rouillon I, Albert S, Chauvin P, Garabedian EN, Couderc R, Odent S, Joannard A, Schmerber S, Delobel B, Leman J, Journel H, Catros H, Lemarechal C, Dollfus H, Eliot MM, Delaunoy JL, David A, Calais C, Drouin-Garraud V, Obstoy MF, Goizet C, Duriez F, Fellmann F, Helias J, Vigneron J, Montaut B, Matin-Coignard D, Faivre L, Baumann C, Lewin P, Petit C, Denoyelle F (2005) GJB2 and GJB6 mutations: genotypic and phenotypic correlations in a large cohort of hearing-impaired patients. Arch Otolaryngol Head Neck Surg 131:481–487

Moisan S, Berlivet S, Ka C, Gac GL, Dostie J, Ferec C (2016) Analysis of long-range interactions in primary human cells identifies cooperative CFTR regulatory elements. Nucleic Acids Res 44:2564–2576

Moisan S, Levon S, Cornec-Le Gall E, Le Meur Y, Audrézet M-P, Dostie J, Férec C (2018) Novel long-range regulatory mechanisms controlling PKD2 gene expression. BMC Genom 19:515

Morton CC, Nance WE (2006) Newborn hearing screening—a silent revolution. N Engl J Med 354:2151–2164

Nora EP, Lajoie BR, Schulz EG, Giorgetti L, Okamoto I, Servant N, Piolot T, Van Berkum NL, Meisig J, Sedat J, Gribnau J, Barillot E, Bluthgen N, Dekker J, Heard E (2012) Spatial partitioning of the regulatory landscape of the X-inactivation centre. Nature 485:381–385

Pallares-Ruiz N, Blanchet P, Mondain M, Claustres M, Roux AF (2002) A large deletion including most of GJB6 in recessive non syndromic deafness: a digenic effect? Eur J Hum Genet 10:72–76

Phillips JE, Corces VG (2009) CTCF: master weaver of the genome. Cell 137:1194–1211

Phillips-Cremins JE, Corces VG (2013) Chromatin insulators: linking genome organization to cellular function. Mol Cell 50:461–474

Phillips-Cremins JE, Sauria ME, Sanyal A, Gerasimova TI, Lajoie BR, Bell JS, Ong CT, Hookway TA, Guo C, Sun Y, Bland MJ, Wagstaff W, Dalton S, Mcdevitt TC, Sen R, Dekker J, Taylor J, Corces VG (2013) Architectural protein subclasses shape 3D organization of genomes during lineage commitment. Cell 153:1281–1295

Pollak A, Mueller-Malesinska M, Skorka A, Kostrzewa G, Oldak M, Korniszewski L, Skarzynski H, Ploski R (2008) GJB2 and hearing

impairment: promoter defects do not explain the excess of monoallelic mutations. J Med Genet 45:607–608
Rao SS, Huntley MH, Durand NC, Stamenova EK, Bochkov ID, Robinson JT, Sanborn AL, Machol I, Omer AD, Lander ES, Aiden EL (2014) A 3D map of the human genome at kilobase resolution reveals principles of chromatin looping. Cell 159:1665–1680
Rodriguez-Paris J, Schrijver I (2009) The digenic hypothesis unraveled: the GJB6 del(GJB6-D13S1830) mutation causes allele-specific loss of GJB2 expression in cis. Biochem Biophys Res Commun 389:354–359
Rodriguez-Paris J, Ballay C, Inserra M, Stidham K, Colen T, Roberson J, Gardner P, Schrijver I (2008) Genetic analysis of presbycusis by arrayed primer extension. Ann Clin Lab Sci 38:352–360
Rodriguez-Paris J, Tamayo ML, Gelvez N, Schrijver I (2011) Allele-specific impairment of GJB2 expression by GJB6 deletion del(GJB6-D13S1854). PLoS One 6:e21665
Rousseau M, Crutchley JL, Miura H, Suderman M, Blanchette M, Dostie J (2014a) Hox in motion: tracking HoxA cluster conformation during differentiation. Nucleic Acids Res 42:1524–1540
Rousseau M, Ferraiuolo MA, Crutchley JL, Wang XQ, Miura H, Blanchette M, Dostie J (2014b) Classifying leukemia types with chromatin conformation data. Genome Biol 15:R60
Roux AF, Pallares-Ruiz N, Vielle A, Faugere V, Templin C, Leprevost D, Artieres F, Lina G, Molinari N, Blanchet P, Mondain M, Claustres M (2004) Molecular epidemiology of DFNB1 deafness in France. BMC Med Genet 5:5
Sanchis-Juan A, Stephens J, French CE, Gleadall N, Megy K, Penkett C, Shamardina O, Stirrups K, Delon I, Dewhurst E, Dolling H, Erwood M, Grozeva D, Stefanucci L, Arno G, Webster AR, Cole T, Austin T, Branco RG, Ouwehand WH, Raymond FL, Carss KJ (2018) Complex structural variants in Mendelian disorders: identification and breakpoint resolution using short- and long-read genome sequencing. Genome Med 10:95
Sanyal A, Lajoie BR, Jain G, Dekker J (2012) The long-range interaction landscape of gene promoters. Nature 489:109–113
Shearer AE, Hildebrand MS, Smith RJH (1993) Hereditary hearing loss and deafness overview. GeneReviews
Smith RJH, Van Camp G (1993) Nonsyndromic hearing loss and deafness, DFNB1. GeneReviews
Smith EM, Lajoie BR, Jain G, Dekker J (2016) Invariant TAD boundaries constrain cell-type-specific looping interactions between promoters and distal elements around the CFTR locus. Am J Hum Genet 98:185–201
Snoeckx RL, Huygen PL, Feldmann D, Marlin S, Denoyelle F, Waligora J, Mueller-Malesinska M, Pollak A, Ploski R, Murgia A, Orzan E, Castorina P, Ambrosetti U, Nowakowska-Szyrwinska E, Bal J, Wiszniewski W, Janecke AR, Nekahm-Heis D, Seeman P, Bendova O, Kenna MA, Frangulov A, Rehm HL, Tekin M, Incesulu A, Dahl HH, Du Sart D, Jenkins L, Lucas D, Bitner-Glindzicz M, Avraham KB, Brownstein Z, Del Castillo I, Moreno F, Blin N, Pfister M, Sziklai I, Toth T, Kelley PM, Cohn ES, Van Maldergem L, Hilbert P, Roux AF, Mondain M, Hoefsloot LH, Cremers CW, Lopponen T, Lopponen H, Parving A, Gronskov K, Schrijver I, Roberson J, Gualandi F, Martini A, Lina-Granade G, Pallares-Ruiz N, Correia C, Fialho G, Cryns K, Hilgert N, Van De Heyning P, Nishimura CJ, Smith RJ, Van Camp G (2005) GJB2 mutations and degree of hearing loss: a multicenter study. Am J Hum Genet 77:945–957
Spielmann M, Mundlos S (2013) Structural variations, the regulatory landscape of the genome and their alteration in human disease. BioEssays 35:533–543
Spielmann M, Mundlos S (2016) Looking beyond the genes: the role of non-coding variants in human disease. Hum Mol Genet 25:R157–R165
Stenson PD, Mort M, Ball EV, Evans K, Hayden M, Heywood S, Hussain M, Phillips AD, Cooper DN (2017) The Human Gene Mutation Database: towards a comprehensive repository of inherited mutation data for medical research, genetic diagnosis and next-generation sequencing studies. Hum Genet 136:665–677
Tayoun ANA, Mason-Suares H, Frisella AL, Bowser M, Duffy E, Mahanta L, Funke B, Rehm HL, Amr SS (2016) Targeted droplet-digital PCR as a tool for novel deletion discovery at the DFNB1 locus. Hum Mutat 37:119–126
Wilch E, Azaiez H, Fisher RA, Elfenbein J, Murgia A, Birkenhager R, Bolz H, Da Silva-Costa SM, Del Castillo I, Haaf T, Hoefsloot L, Kremer H, Kubisch C, Le Marechal C, Pandya A, Sartorato EL, Schneider E, Van Camp G, Wuyts W, Smith RJ, Friderici KH (2010) A novel DFNB1 deletion allele supports the existence of a distant cis-regulatory region that controls GJB2 and GJB6 expression. Clin Genet 78:267–274
Wilcox SA, Saunders K, Osborn AH, Arnold A, Wunderlich J, Kelly T, Collins V, Wilcox LJ, Mckinlay Gardner RJ, Kamarinos M, Cone-Wesson B, Williamson R, Dahl HH (2000) High frequency hearing loss correlated with mutations in the GJB2 gene. Hum Genet 106:399–405
Wu X, Wang Y, Sun Y, Chen S, Zhang S, Shen L, Huang X, Lin X, Kong W (2014) Reduced expression of Connexin26 and its DNA promoter hypermethylation in the inner ear of mimetic aging rats induced by d-galactose. Biochem Biophys Res Commun 452:340–346
Zelante L, Gasparini P, Estivill X, Melchionda S, D'Agruma L, Govea N, Mila M, Monica MD, Lutfi J, Shohat M, Mansfield E, Delgrosso K, Rappaport E, Surrey S, Fortina P (1997) Connexin26 mutations associated with the most common form of non-syndromic neurosensory autosomal recessive deafness (DFNB1) in Mediterraneans. Hum Mol Genet 6:1605–1609